

## Lattice dynamics of $\alpha$ carbon monoxide\*

Barbara Okray Hall<sup>†</sup> and Hubert M. James

*Purdue University, West Lafayette, Indiana 60439*

(Received 1 December 1975)

Previous calculations of the lattice dynamics of  $\alpha$ -CO have neglected the mass asymmetry of the molecules and have assumed a centrosymmetric  $Pa3$  structure for the crystal rather than the observed  $P2_13$  structure. Coupling between translational and librational lattice modes has been ignored and anharmonic effects have not been considered in detail. This work includes these factors in lattice-dynamics calculations for  $\alpha$ -CO and examines their effect on computed frequencies for  $\vec{k} = 0$ . Anharmonic effects are treated in the quasiharmonic approximation of Boccara and Sarma. The model assumes rigid mass-asymmetric molecules, end-for-end ordering, and molecular pair interactions consisting of a point quadrupole interaction with adjustable quadrupole moment  $Q$  and an atom-atom Lennard-Jones (6-12) interaction with three adjustable parameters  $\sigma$ ,  $\epsilon$ , and  $b$ , an effective bond length. Dipole interactions are neglected. Parameters were adjusted to fit the observed cohesive energy and lattice constant, and to give an optimal representation of the seven lattice frequencies in the Raman and infrared spectra. Calculations were performed in both harmonic and quasiharmonic approximations for bond lengths  $b = 0$  and 0.282 Å. Frequencies calculated in the quasiharmonic approximation for the two bond lengths give a much better fit to the observed spectrum than the corresponding harmonic results, and for a given approximation the one-center potential yields a better fit than the two center. The  $P2_13$  distortion predicted by the model in the harmonic approximation is very small and in a direction opposite to that observed by Vegard, and in the quasiharmonic approximation is either in the direction opposite to that measured or in the observed direction but less than 20% of the observed magnitude. Comparison of the frequency spectra for symmetric and asymmetric molecules indicates that the mass dissymmetry has only a slight effect on the calculated frequencies.

### I. INTRODUCTION

Pauling<sup>1</sup> initiated the investigation of rotational motions of molecules in crystals with the discussion of the wave equation for a diatomic molecule in a crystal field. He concluded that, in the limiting case of strong intermolecular forces and large molecular moments of inertia, the molecules tended to oscillate about certain equilibrium orientations, whereas, in the case of weak forces and small moments of inertia the rotational motion approached that of a free molecule. Although the analysis of molecular motions in crystals has since become more sophisticated, the classification as oscillatory or rotational is still useful and serves to reflect the approaches taken in treating the dynamics of a particular crystal. For example, hydrogen and deuterium belong to the rotational category, and general treatments of their dynamic properties start with free-rotor wave functions and the orientational potential treated as a weak perturbation. Molecules in naphthalene and anthracene oscillate, and descriptions of their motions begin with harmonic-oscillator wave functions. Intermediate cases are represented by  $\alpha$ -CO, the subject of this work, and  $\alpha$ -N<sub>2</sub>, which is similar in structure and properties.

The lattice frequencies of  $\alpha$ -N<sub>2</sub> and  $\alpha$ -CO have been calculated using effective-field theories<sup>2-4</sup> and the harmonic approximation.<sup>5-9</sup> The major emphasis has been toward finding a form for the anisotropic intermolecular potential which de-

scribes the librational spectrum well. All the models used have assumed the  $Pa3$  structure for both crystals, and rigid symmetric molecules. Except for the calculations of Shinoda and Enokido<sup>7</sup> all of the work has been done on  $\alpha$ -N<sub>2</sub>; results quoted for  $\alpha$ -CO have been obtained by simply adjusting parameters in models of  $\alpha$ -N<sub>2</sub>.

The main conclusion to be drawn from previous calculations is that a clearer understanding of the dynamics of these crystals is necessary. Anharmonic effects are generally considered important as evidenced by the thermal and spectral data for the crystal but no attempts have been made to include them in calculations. Translational-librational coupling has not been treated in detail, and the correct structure for these crystals has been ignored. The purpose of this work was to include these factors in lattice-dynamics calculations for  $\alpha$ -CO and examine their effect on the computed frequencies.

Lattice-dynamics calculations were done in both the harmonic and quasiharmonic approximations; anharmonic effects are included in part when the latter is used. The problem, however, was complicated by the lack of a good potential energy for interaction of two CO molecules. There is no agreement on the exact form of the intermolecular pair potential or on the values of the parameters for any particular form, so in this work the potential parameters were adjusted to give the best representation of experimental data possible for the approximation used. The data included the lattice

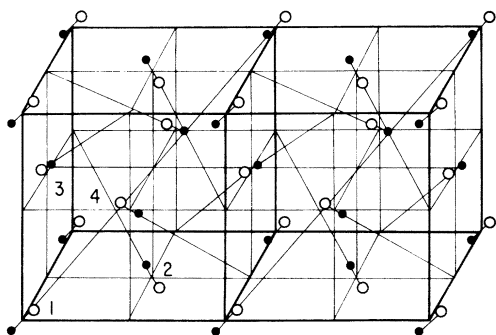


FIG. 1. Crystal structure for  $\alpha$ -CO. Two unit cells are shown with positions of oxygen atoms indicated by open circles.

constant, the cohesive energy, and the seven lattice frequencies measured in the Raman and infrared spectra. The results for the two approximations were compared in order to evaluate the effect of the choice of approximation on both the frequency calculation and the potential parameters.

## II. MODEL OF $\alpha$ -CO

The  $\alpha$ -carbon-monoxide crystal is primitive cubic with four molecules in the basis, as shown in Fig. 1, and belongs to space group  $P2_13$ . This structure is closely related to the more symmetric  $Pa3$  structure assumed in previous studies of CO, and a description of the latter will serve to clarify the details of the former.

In the equilibrium configuration of the  $Pa3$  structure, the centers of the molecules are located at the corners and face centers of a cube and the internuclear axes are oriented along the body diagonals. The lattice is composed of four interpenetrating simple cubic lattices, each made up of molecules with a particular equilibrium axial orientation, parallel to one of the body diagonals of the cube. Symmetry operations which take the crystal into itself include lattice translations, threefold rotations about each of the molecular axes, screw operations consisting of twofold rotations about the crystal axes followed by nonprimitive translations, inversion, and combinations of these operations.

Inclusion of an end-for-end dissymmetry of the molecule reduces the structure to  $P2_13$ . Specification of the end-for-end ordering on a single sublattice is sufficient to determine the ordering on all the sublattices if the threefold axes of the  $Pa3$  structure are assumed to be maintained. The directional sense thus acquired by the molecular axes will be taken as positive when going from the carbon atom to the oxygen atom. Inversion is no longer a crystal symmetry operation.

The  $Pa3$  space group also reduces to the  $P2_13$

space group if each molecule is displaced along its C-O axis, the magnitude and sense of the displacement being the same for all sublattices. This displacement will be referred to as the  $P2_13$  distortion,  $s$ . Vegard<sup>10</sup> found the displacement to be positive in CO, in the direction of the oxygen atom.

The equilibrium positions of the carbon and oxygen atoms in the  $P2_13$  structure are given in Table I. The coordinates refer to a Cartesian system with axes parallel to the cube edges and origin at the center of a molecule on sublattice 1 when the distortion is zero. The unit of distance is the length of the cube edge.

In the model the intramolecular nuclear separation is assumed to be fixed at the experimentally determined mean internuclear separation. The centers of mass are thus displaced from the midpoints of the lines joining the nuclei in the direction of the oxygen nuclei. It should be noted that when the crystal is given the distortion measured by Vegard, the centers of mass are displaced even further from the face-centered-cubic sites.

There are three primary interactions between two carbon monoxide molecules: (a) an attractive van der Waals interaction, (b) a repulsive short-range interaction, and (c) a quadrupole-quadrupole electrostatic interaction. The first two will be represented by an atom-atom (6-12) Lennard-Jones potential, which is a sum of interactions between the four nonbonded pairs of atoms in the two molecules. The interaction has the form,

$$V^{LJ} = \epsilon \sum_{\alpha=1}^4 \left[ \left( \frac{\sigma}{R_{\alpha}} \right)^{12} - \left( \frac{\sigma}{R_{\alpha}} \right)^6 \right], \quad (2.1)$$

where  $R_{\alpha}$  is the distance between two nonbonded atoms. The two parameters  $\epsilon$  and  $\sigma$  are assumed to be equal for the C-O, O-O, and C-C interactions.

The quantum-mechanical calculation of the charge distribution of CO by Nesbet<sup>11</sup> indicates that the contours of constant charge density for the molecule are nearly symmetric and similar to those for  $N_2$ .<sup>12</sup> Thus the centers of interaction

TABLE I. Equilibrium positions of the carbon and oxygen atoms in the  $P2_13$  structure.  $P2_13$  distortion  $s = \sqrt{3}(v-w)/2$ .

Sublattice	Equilibrium orientation	Oxygen	Carbon
1	[111]	( $v, v, v$ )	( $-w, -w, -w$ )
2	[1-1-1]	( $\frac{1}{2} + v, \frac{1}{2} - v, -v$ )	( $\frac{1}{2} - w, \frac{1}{2} + w, w$ )
3	[-11-1]	( $-v, \frac{1}{2} + v, \frac{1}{2} - v$ )	( $w, \frac{1}{2} - w, \frac{1}{2} + w$ )
4	[-1-11]	( $\frac{1}{2} - v, -v, \frac{1}{2} + v$ )	( $\frac{1}{2} + w, w, \frac{1}{2} - w$ )

of the two atoms in the molecule can be located at the nuclei or at points symmetrically placed about the midpoint of the line joining the nuclei. The distance  $b$  between the carbon and oxygen centers of the interaction on the molecule is then an "effective" bond length which can be considered an adjustable potential parameter. The use of an effective bond length shorter than the measured internuclear separation is physically reasonable, since it is the electronic structure, not the internuclear separation, which determines the attractive van der Waals forces and the distances at which the repulsive interaction dominates.

The atom-atom form of the Lennard-Jones potential has isotropic and anisotropic terms and so influences both the positions of the molecules and their orientation.

The interaction between the permanent quadrupole moments of two carbon monoxide molecules is given by

$$V^Q = \frac{3}{4} (Q^2/R_{12}^2) [1 - 5(\hat{n}_1 \cdot \hat{R}_{12})^2 - 5(\hat{n}_2 \cdot \hat{R}_{12})^2 + 35(\hat{n}_1 \cdot \hat{R}_{12})^2 (\hat{n}_2 \cdot \hat{R}_{12})^2 - 15(\hat{n}_1 \cdot \hat{n}_2)(\hat{n}_1 \cdot \hat{R}_{12})(\hat{n}_2 \cdot \hat{R}_{12})], \quad (2.2)$$

where  $Q$  is the quadrupole moment,  $\hat{n}_i$  is the unit vector along the C-O axis of molecule  $i$ , and  $\hat{R}_{12}$  is the unit vector along the line joining the centers of the molecules. Because of the complex angular dependence of the quadrupole pair interaction, large cancellations occur when this potential is summed over the crystal lattice, and its contribution to the crystal energy tends to be small. Its primary effect is to orient the molecules.

Carbon monoxide is a polar molecule, possessing a permanent dipole moment, and a dipole-dipole interaction exists between pairs of molecules. The value of the dipole moment has been calculated by Burrus<sup>13</sup> from Stark-effect measurements as 0.112 D. This small value means that the contributions of the nuclei and the electrons to the moment nearly cancel and the molecule is approximately electrically symmetric. In the crystal structure  $P2_13$ , the arrangement of the equilibrium orientations of the molecules minimizes the electrostatic energy of the quadrupole interaction; this configuration also makes the contribution of the dipole interaction to the crystal energy small.<sup>14</sup> For these reasons, the dipole interaction is neglected here.

The energy required to reverse a dipole in an otherwise ordered crystal is equal to  $kT$  at about 5 K, and thus considerable end-for-end ordering could be expected at this temperature. The barrier to end-for-end reversal, however, is estimated as 1700 cal/mole and the rate of ordering by thermal excitation is negligible.<sup>15</sup> Tunneling provides a possible mechanism, but heat-capacity

measurements to 2.5 K show no transition.<sup>16</sup> Calorimetric studies of CO reveal a residual entropy owing to partial end-for-end disorder down to the lowest measured temperatures.<sup>16,17</sup> Because of the difficulty in dealing with a disordered crystal, however, perfect ordering is assumed in the model used here, with the molecular axes in the sense determined by Vegard.

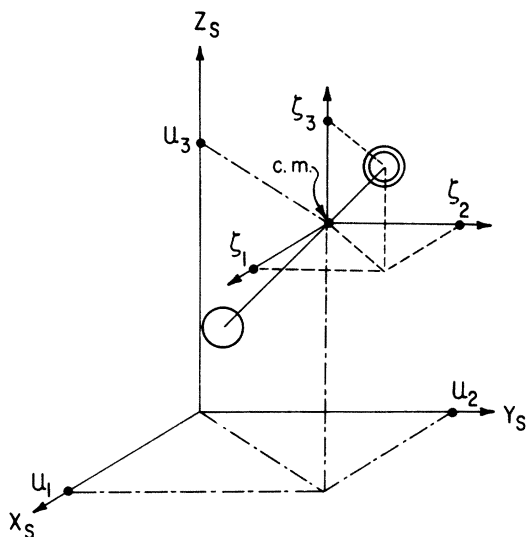
Pairwise additivity of molecular interactions is assumed, so that the total crystal potential is a sum over all pair interactions. Neglect of three-body interactions seems justified, since studies for solid argon show that their inclusion changes the crystal energy by only a few percent.<sup>18</sup> Kohin refers to a calculation by Lupton which gives the correction to the crystal energy of CO owing to three-body interactions as 1.5%.

Dielectric screening is also ignored in the model. All of the interactions are of relatively short range and can be considered negligible at distances of two or three unit-cell lengths. The main contributions come from first and second neighbors where dielectric screening is not expected to be effective.

### III. MOLECULAR COORDINATES

In the mathematical treatment of the lattice dynamics of  $\alpha$ -CO, it is convenient to use two types of coordinate systems; one based on the cubic nature of the crystal lattice and the other related to the local equilibrium orientations of the molecules. The lattice or crystal coordinate system has axes parallel to the edges of the cubic unit cell, while the local or site coordinate system for each molecule is defined so that the  $z$  axis is along the equilibrium internuclear axis with the positive direction toward the oxygen nucleus and the origin is at the molecular center of mass. There is some arbitrariness in the choice of  $x$  and  $y$  axes; if they are chosen to be symmetric about the diagonal plane of the cube containing the  $z$  axis, however, the crystal potential is symmetric in the two coordinates. Once a site-coordinate system is set up for molecules on one sublattice, the site systems for the remaining sublattices are determined by the condition that the three screw operations take the site coordinate axes of one sublattice into those of another. The components of a vector in the lattice system are related to those in the  $\kappa$  site system by an orthogonal transformation.

Local site coordinates of the type discussed here have been used in the description of librational excitations in hydrogen<sup>19,20</sup> and  $\alpha$ -N<sub>2</sub>.<sup>3,6,21</sup> Full lattice-dynamics calculations for nearly harmonic crystals which include both translational and orientational degrees of freedom have only been done using the crystal coordinate system.<sup>8,9,22,23</sup> In the present work the site coordinates have the advan-

FIG. 2. Molecular projection coordinates  $\xi_1$  and  $\xi_2$ .

tage over the crystal coordinates that they transform more simply under the symmetry operations of the crystal. In addition, their use simplifies the description of molecular displacements from equilibrium.

Five coordinates are needed to specify the instantaneous position and orientation of a rigid CO molecule: three Cartesian coordinates to locate the center of mass and two coordinates to fix the orientation of the symmetry axis. The angular orientational coordinates used by various authors<sup>6,8,9,21</sup> have the disadvantage that they do not transform linearly under the symmetry operations of the crystal. The direction cosines used by Walmsley and Pople<sup>22</sup> transform linearly, but there are three direction cosines and only two are independent. The inclusion of the extra coordinate leads to formal problems and requires care in handling. The displacement coordinates used in this work avoid the problem of redundant coordinates and transform linearly under the crystal symmetry operations.

The projections of the instantaneous vector from the center of mass to the oxygen nucleus on the  $x$  and  $y$  axes of the site coordinate system are here used to define the instantaneous orientation of a molecule. These projections are the  $x$  and  $y$  coordinates of the oxygen nucleus in a coordinate system with axes parallel to the site axes, but translated so that its origin is at the instantaneous c. m. position as illustrated in Fig. 2.

Since the molecule is treated as rigid, the projection along the  $z$  axis can be expressed in terms of those along the  $x$  and  $y$  axes. If  $d$  is the c. m. to O distance, and  $\xi_i$  is a projection along the  $i$  axis, then

$$\xi_3 = \pm d \left( 1 - \frac{\xi_1^2 + \xi_2^2}{d^2} \right)^{1/2}. \quad (3.1)$$

The positive sign will always be chosen, since orientational ordering is assumed. In the equilibrium configuration  $\xi_1$  and  $\xi_2$  are zero, and their instantaneous values measure displacements from this orientation.

The instantaneous coordinates of the c. m. in the local site system are displacements from the equilibrium position at the origin. These three Cartesian coordinates  $u_1(l\kappa)$ ,  $u_2(l\kappa)$ ,  $u_3(l\kappa)$  and the two projections  $\xi_1(l\kappa)$  and  $\xi_2(l\kappa)$  describe the position and orientation of molecule  $(l\kappa)$ , where the index  $l$  indicates the unit cell and the index  $\kappa$  the sublattice on which it is found.

The crystal potential is the sum of all pair potentials

$$\Phi = \frac{1}{2} \sum_{\substack{l\kappa \\ l'\kappa'}} V(l\kappa; l'\kappa')$$

with  $V(l\kappa; l\kappa) = 0$  for all  $(l\kappa)$ . Expanding  $\Phi$  in a Taylor's series in the molecular displacement coordinates gives

$$\begin{aligned} \Phi &= \Phi_0 + \frac{1}{2!} \sum_{\substack{l\kappa\alpha \\ l'\kappa'\beta}} \Phi_{\alpha\beta}(l\kappa; l'\kappa') u_\alpha(l\kappa) u_\beta(l'\kappa') \\ &+ \frac{1}{3!} \sum_{\substack{l\kappa\alpha \\ l'\kappa'\beta \\ l''\kappa''\gamma}} \Phi_{\alpha\beta\gamma}(l\kappa; l'\kappa'; l''\kappa'') u_\alpha(l\kappa) u_\beta(l'\kappa') u_\gamma(l''\kappa'') \\ &+ \frac{1}{4!} \sum_{\substack{l\kappa\alpha \\ l'\kappa'\beta \\ l''\kappa''\gamma \\ l'''\kappa'''\delta}} \Phi_{\alpha\beta\gamma\delta}(l\kappa; l'\kappa'; l''\kappa''; l'''\kappa''') \\ &\times u_\alpha(l\kappa) u_\beta(l'\kappa') u_\gamma(l''\kappa'') u_\delta(l'''\kappa'''). \end{aligned} \quad (3.2)$$

The sum over  $\alpha$  and  $\beta$  runs from 1-5 with  $u_4(l\kappa) \equiv \xi_1(l\kappa)$  and  $u_5(l\kappa) \equiv \xi_2(l\kappa)$ . The expansion coefficients are derivatives of the crystal potential with respect to the displacement coordinates, evaluated for the equilibrium configuration. For example,

$$\Phi_{\alpha\beta}(l\kappa; l'\kappa') = \left. \frac{\partial^2 \Phi}{\partial u_\alpha(l\kappa) \partial u_\beta(l'\kappa')} \right|_{\text{eq}}$$

The expansion coefficients or force constants can be expressed in terms of derivatives of pair potentials, and analytic forms are easily obtained. Since the potential has the full space-group symmetry and is invariant to rigid-body translations and rotations, large numbers of the force constants are related and only a limited number need be explicitly evaluated.

#### IV. HARMONIC APPROXIMATION

The treatment of lattice dynamics in the harmonic approximation is well known, and many texts treat the subject in detail.<sup>24</sup> The approxi-

mation consists of truncating the Taylor's series expansion of the potential after the second-order terms. If the kinetic energy is also in quadratic form, the Hamiltonian is then recognizable as that of a system of coupled harmonic oscillators. The oscillators are uncoupled by a unitary transformation to normal-mode coordinates which can be written in terms of the molecular site coordinates as

$$Q(\vec{k}j) = N^{-1/2} \sum_{I\kappa\alpha} M_\alpha^{1/2} W_\alpha^*(\kappa|\vec{k}j) u_\alpha(I\kappa) e^{-i\vec{k}\cdot\vec{z}(I\kappa)}, \quad (4.1)$$

where  $\vec{k}$  is a vector in the Brillouin zone,  $j$  is a branch index,  $N$  is the number of unit cells in the crystal, and  $M_\alpha$ , the generalized mass, is equal to the mass of the molecule if  $\alpha = 1, 2$ , or  $3$ , and equal to  $I/d^2$  (where  $I$  is the moment of inertia) if  $\alpha = 4$  or  $5$ . The components  $W_\alpha(\kappa|\vec{k}j)$  of the 20-component polarization vector satisfy the orthogonality conditions:

$$\sum_{\kappa\alpha} W_\alpha^*(\kappa|\vec{k}j) W_\alpha(\kappa|\vec{k}j') = \delta_{jj'},$$

$$\sum_j W_\alpha^*(\kappa|\vec{k}j) W_\beta(\kappa'|\vec{k}j) = \delta_{\kappa\kappa'} \delta_{\alpha\beta}.$$

Expressed in the normal-mode coordinates, the ground-state wave function for the system is

$$\Psi_{\text{gs}} = A \exp\left(-\frac{1}{2\hbar} \sum_{\vec{k}j} \omega_{\vec{k}j} Q(\vec{k}j) Q^*(\vec{k}j)\right), \quad (4.2)$$

where  $\omega_{\vec{k}j}$  is the frequency of the normal mode. In terms of the molecular coordinates

$$\Psi_{\text{gs}} = A \exp\left(-\hbar^{-2} \sum_{\substack{I\kappa\alpha \\ I'\kappa'\beta}} \rho_{\alpha\beta}(I\kappa; I'\kappa') u_\alpha(I\kappa) u_\beta(I'\kappa')\right) \quad (4.3)$$

and the expression

$$\rho_{\alpha\beta}(I\kappa; I'\kappa') = \frac{\hbar}{2N} \sum_{\vec{k}j} \omega_{\vec{k}j} (M_\alpha M_\beta)^{1/2} W_\alpha(\kappa|\vec{k}j) W_\beta^*(\kappa'|\vec{k}j) \times e^{i\vec{k}\cdot[\vec{z}(I\kappa) - \vec{z}(I'\kappa')]} \quad (4.4)$$

is the equal-time momentum correlation function for  $T=0$ . The wavefunction given in Eq. (4.3) is no longer a product function; the argument of the Gaussian contains cross terms between different site coordinates and is called a correlated Gaussian.<sup>25-27</sup>

The molecular coordinates can be treated as the components of a  $20N$  vector  $\vec{u}$ , with the momentum correlation functions  $\rho_{\alpha\beta}(I\kappa; I'\kappa')$  forming a  $20N \times 20N$  matrix  $\underline{\rho}$ . The exponent in Eq. (4.3) is then  $-\hbar^{-2} \vec{u}^T \cdot \underline{\rho} \cdot \vec{u}$ . The matrix  $\underline{\rho}$  is the inverse of the displacement correlation matrix  $\underline{\sigma}$ , whose elements are the equal-time displacement correlation functions for zero temperature:

$$\sigma_{\alpha\beta}(I\kappa; I'\kappa') = \langle u_\alpha(I\kappa) u_\beta(I'\kappa') \rangle = \frac{\hbar}{2N} (M_\alpha M_\beta)^{-1/2} \sum_{\vec{k}j} W_\alpha(\kappa|\vec{k}j) \omega_{\vec{k}j}^{-1} W_\beta^*(\kappa'|\vec{k}j) \times e^{i\vec{k}\cdot[\vec{z}(I\kappa) - \vec{z}(I'\kappa')]} \quad (4.5)$$

The symbol  $\langle \rangle$  indicates an average over the ground-state wave function.

#### A. Quadratic form for the kinetic energy

The quantum-mechanical angular momentum operator  $\mathcal{L}^2$  for a linear molecule is

$$\mathcal{L}^2 = -\hbar^2 \left[ \frac{1}{\sin\theta} \frac{\partial}{\partial\theta} \left( \sin\theta \frac{\partial}{\partial\theta} \right) + \frac{1}{\sin^2\theta} \frac{\partial^2}{\partial\phi^2} \right], \quad (4.6)$$

which when written in terms of the projection coordinates becomes

$$\mathcal{L}^2 = -\hbar^2 \left( (d^2 - \zeta_1^2) \frac{\partial^2}{\partial\zeta_1^2} + (d^2 - \zeta_2^2) \frac{\partial^2}{\partial\zeta_2^2} - 2\zeta_1 \frac{\partial}{\partial\zeta_1} - 2\zeta_2 \frac{\partial}{\partial\zeta_2} - 2\zeta_1\zeta_2 \frac{\partial^2}{\partial\zeta_1\partial\zeta_2} \right). \quad (4.7)$$

If the displacement of the molecules from the equilibrium orientation is small, the terms containing displacements as multipliers can be neglected, and the operator is approximately

$$\mathcal{L}^2 \approx -\hbar^2 d^2 \left( \frac{\partial^2}{\partial\zeta_1^2} + \frac{\partial^2}{\partial\zeta_2^2} \right). \quad (4.8)$$

The kinetic energy for the crystal will correspondingly be approximated by

$$T = T_{\text{trans}} + T_{\text{lib}} = \frac{M}{2} \sum_{\substack{I\kappa \\ \alpha=1,2,3}} \dot{u}_\alpha^2(I\kappa) + \frac{I}{2d^2} \sum_{\substack{I\kappa \\ \alpha=4,5}} \dot{u}_\alpha^2(I\kappa), \quad (4.9)$$

where the second term is the classical equivalent of Eq. (4.8). In  $\alpha$ -CO, since large-angle librations are not negligible, the validity of this approximation is open to question. Numerical estimates indicate that the contribution of the neglected terms to the ground-state kinetic energy is no larger than 6% of the retained terms.

#### B. Dynamical matrix

With the kinetic energy of the crystal in quadratic form, the equations of motion for the molecules are

$$M_\alpha \ddot{u}_\alpha(I\kappa) = - \sum_{I'\kappa'\beta} \Phi_{\alpha\beta}(I\kappa; I'\kappa') u_\beta(I'\kappa'). \quad (4.10)$$

This system of  $20N$  equations can be partially uncoupled by considering plane waves of the form

$$u_\alpha(I\kappa) = M_\alpha^{-1/2} W_\alpha(\kappa|\vec{k}j) e^{-i[\omega t - \vec{k}\cdot\vec{z}(I\kappa)]}. \quad (4.11)$$

If one defines a dynamical matrix  $\underline{C}(\vec{k})$  as

$$C_{\alpha\beta}(\kappa\kappa'|\vec{k}) = (M_\alpha M_\beta)^{-1/2} \sum_{l'} \phi_{\alpha\beta}(l\kappa; l'\kappa') \\ \times e^{-i\vec{k}\cdot[\vec{x}(l\kappa) - \vec{x}(l'\kappa')]} , \quad (4.12)$$

the equations of motion take the form

$$\omega_{\vec{k}j}^2 W_\alpha(\kappa|\vec{k}j) = \sum_{\beta\kappa'} C_{\alpha\beta}(\kappa\kappa'|\vec{k}) W_\beta(\kappa'|\vec{k}j) . \quad (4.13)$$

Equation (4.13) gives a set of 20 linear equations for each of  $N$  wave vectors  $\vec{k}$ . These can be solved by standard techniques for the squares of the normal-mode frequencies that correspond to the different  $j$ , and for the associated polarization vectors.

### V. QUASIHARMONIC APPROXIMATION

The treatment of anharmonic crystals can be developed from many viewpoints including perturbation theory, Green's-function techniques, and variational procedures<sup>28-33</sup>; the approaches are reviewed and referenced by Werthamer.<sup>28</sup> The quasiharmonic approximation used here was developed by Boccara and Sarma,<sup>32</sup> and has the advantage of using many results of the harmonic theory.

In the quasiharmonic approximation the anharmonic Hamiltonian of the system

$$H_{\text{exact}} = T + V_a \quad (5.1)$$

is replaced by a trial harmonic Hamiltonian

$$H_{\text{trial}} = H_h + E_0 = T + V_h + E_0 , \quad (5.2)$$

which has the symmetry of the original but is otherwise general. The subscript  $a$  refers to anharmonic and  $h$  to harmonic;  $E_0$  is a constant that will be discussed later. The solution of the wave equation with the trial Hamiltonian is known; the ground-state wave function is the correlated Gaussian of Eq. (4.3). This is to serve as an approximation to the exact ground-state wave function. The approximate free energy  $F_h$  of the harmonic system, evaluated using the trial Hamiltonian, is given by

$$F_h = k_B T \sum_{\vec{k}j} \ln \left( 2 \sinh \frac{\hbar\omega_{\vec{k}j}}{2k_B T} \right) + E_0 , \quad (5.3)$$

where  $k_B$  is the Boltzmann constant and  $T$  is the temperature. The first term is the free energy of the system of trial harmonic oscillators and depends on the parameters of  $V_h$  through the vibrational frequencies  $\omega_{\vec{k}j}$ . Using the Bogoliubov inequality,<sup>34</sup> the free energy  $F_h$  can be related to the exact free energy  $F$  of the system:

$$F \leq F_h + \langle H_{\text{exact}} - H_{\text{trial}} \rangle_{\text{trial}} . \quad (5.4)$$

The notation  $\langle \rangle_{\text{trial}}$  indicates an average over the canonical ensemble for the trial harmonic system at any given temperature  $T$ . When  $T=0$  this aver-

age reduces to an average over the trial ground-state wave function, and  $F$  and  $F_h$  are the ground-state energies of the exact and trial systems. If the ensemble averages of the exact and trial Hamiltonians are equal, the second term in Eq. (5.4) vanishes. By setting the constant

$$E_0 = \langle V_a \rangle_{\text{trial}} - \langle V_h \rangle_{\text{trial}} , \quad (5.5)$$

this condition is met, and  $F \leq F_h$ .

To get the best harmonic approximation to the exact Hamiltonian, the parameters in the trial Hamiltonian are adjusted so as to minimize the value of  $F_h$  computed with that Hamiltonian. This variational procedure tends to give a good overall fit of the harmonic spectrum to the observed one. Each normal mode frequency enters the calculation with a weight factor which is related to the degree of excitation of that normal mode at the temperature under consideration, and the form of  $H_{\text{trial}}$  thus depends on the temperature. When the calculation is made for  $T=0$ , all modes are still taken into account, since each has a zero-point vibration. In this case the ground-state wave function for the optimum  $H_h$  is the best approximation to the exact ground-state wave function in the sense of the usual variational method, within the manifold of correlated-Gaussian functions. Eigenfunctions of  $H_h$  could be used to compute excitation frequencies from the exact Hamiltonian, as

$$\hbar\omega_{\text{ex}} = \langle H_{\text{exact}} \rangle_{\text{excit}} - \langle H_{\text{exact}} \rangle_{\text{gs}} , \quad (5.6)$$

where the averages are taken over the approximate wave functions for the ground-state and a singly-excited state of the system. It can be shown that this yields just the normal mode frequencies for the harmonic  $H_h$  rather than a more accurate approximation.

The anharmonic potential assumed in this work is given in Eq. (3.2). The trial harmonic Hamiltonian has the form

$$H_{\text{trial}} = T + \frac{1}{2!} \sum_{\substack{l\kappa\alpha \\ l'\kappa'\beta}} \Gamma_{\alpha\beta}(l\kappa; l'\kappa') u_\alpha(l\kappa) u_\beta(l'\kappa') + E_0 . \quad (5.7)$$

The ensemble average of the product of two displacement coordinates over a harmonic wave function is given by Maradudin, Montroll, Weiss, and Ipatova<sup>24</sup>; their result can be rewritten in terms of the eigenvalues and eigenvectors of the dynamical matrix  $\underline{C}(\vec{k})$  constructed from the trial Hamiltonian,

$$\sigma_{\alpha\beta}^T(l\kappa; l'\kappa') \equiv \langle u_\alpha(l\kappa) u_\beta(l'\kappa') \rangle_{\text{trial}} \\ = - \frac{\hbar}{2N(M_\alpha M_\beta)^{1/2}} \sum_{\vec{k}j} \coth \left( \frac{\beta\hbar\omega_{\vec{k}j}}{2} \right) W_\alpha(\kappa|\vec{k}j) \\ \times W_\beta(\kappa'|\vec{k}j) \omega_{\vec{k}j}^{-1} e^{-i\vec{k}\cdot[\vec{x}(l\kappa) - \vec{x}(l'\kappa')]} , \quad (5.8)$$

where  $\beta$  is the temperature factor  $(k_B T)^{-1}$ . This

expression is the equal-time displacement correlation function for finite  $T$ . Similar averages of products of three and four  $u$ 's appear in the calculation. It can be shown that

$$\sigma_{\alpha\beta\gamma}^T(l\kappa; l'\kappa'; l''\kappa'') = 0 \quad (5.9)$$

for all values of the indices, and that

$$\begin{aligned} \sigma_{\alpha\beta\gamma\delta}^T(l\kappa; l'\kappa'; l''\kappa''; l'''\kappa''') \\ = \sigma_{\alpha\beta}^T(l\kappa; l'\kappa') \sigma_{\gamma\delta}^T(l''\kappa''; l'''\kappa''') \\ + \sigma_{\alpha\gamma}^T(l\kappa; l''\kappa'') \sigma_{\beta\delta}^T(l'\kappa'; l'''\kappa''') \\ + \sigma_{\alpha\delta}^T(l\kappa; l'''\kappa''') \sigma_{\beta\gamma}^T(l'\kappa'; l''\kappa''). \end{aligned} \quad (5.10)$$

Using Eqs. (5.5), (5.9), and (5.10) the constant  $E_0$  can be written

$$\begin{aligned} E_0 = \Phi_0 + \frac{1}{2!} \sum_{l'\kappa'\alpha} [\Phi_{\alpha\beta}(l\kappa; l'\kappa') - \Gamma_{\alpha\beta}(l\kappa; l'\kappa')] \\ + \frac{3}{4!} \sum_{\substack{l'\kappa'\beta \\ l''\kappa''\gamma \\ l'''\kappa'''\delta}} \Phi_{\alpha\beta\gamma\delta}(l\kappa; l'\kappa'; l''\kappa''; l'''\kappa''') \\ \times \sigma_{\alpha\beta}^T(l\kappa; l'\kappa') \sigma_{\gamma\delta}^T(l''\kappa''; l'''\kappa'''). \end{aligned} \quad (5.11)$$

From Eq. (5.11) it can be seen that  $E_0$  is a function of both the physical properties of the crystal, contained in the potential derivatives, and the parameters  $\Gamma_{\alpha\beta}(l\kappa; l'\kappa')$  of the trial Hamiltonian. The correlation functions  $\sigma_{\alpha\beta}^T(l\kappa; l'\kappa')$  depend implicitly on the trial force constants through the dynamical matrix.

The optimum values of the trial force constants are obtained by minimizing the free energy  $F_h$  with respect to independent variations of the trial force constants and the correlation functions, despite the fact that these quantities are interrelated. The equations, if they are soluble, are sufficient to ensure the stationary character of  $F_h$ , and they are in fact self-consistent.

The trial free energy can be obtained by combining Eqs. (5.3) and (5.11). Taking the derivative of  $F_h$  with respect to  $\Gamma_{\alpha\beta}(l\kappa; l'\kappa')$  while holding constant the correlation functions and the other trial force constants, and requiring the result to vanish, one gets

$$\begin{aligned} \frac{\partial F_h}{\partial \Gamma_{\alpha\beta}(l\kappa; l'\kappa')} = \frac{\hbar}{2} \sum_{\mathbf{f}j} \coth\left(\frac{\hbar\omega_{\mathbf{f}j}}{2k_B T}\right) \frac{\partial \omega_{\mathbf{f}j}}{\partial \Gamma_{\alpha\beta}(l\kappa; l'\kappa')} \\ - \frac{N}{2} \sigma_{\alpha\beta}^T(l\kappa; l'\kappa') = 0, \end{aligned} \quad (5.12)$$

the factor  $N$  arising from translationally equivalent pairs. Equation (5.12) can be shown to be equivalent to Eq. (5.8). The derivative with respect to the correlation function  $\sigma_{\alpha\beta}^T(l\kappa; l'\kappa')$  is

$$\frac{\partial F_h}{\partial \sigma_{\alpha\beta}^T(l\kappa; l'\kappa')} = \frac{\partial E}{\partial \sigma_{\alpha\beta}^T(l\kappa; l'\kappa')} = 0, \quad (5.13)$$

and yields the condition

$$\begin{aligned} \Gamma_{\alpha\beta}(l\kappa; l'\kappa') = \Phi_{\alpha\beta}(l\kappa; l'\kappa') + \frac{1}{2!} \\ \times \sum_{\substack{l''\kappa''\delta \\ l'''\kappa'''\delta}} \Phi_{\alpha\beta\gamma\delta}(l\kappa; l'\kappa'; l''\kappa''; l'''\kappa''') \\ \times \sigma_{\gamma\delta}^T(l''\kappa''; l'''\kappa'''). \end{aligned} \quad (5.14)$$

The right-hand side of Eq. (5.14) is the thermal average of a second derivative of the anharmonic potential, and yields a different force constant for every temperature, with a value that may vary widely from the harmonic one if the molecular displacements are large or the derivative is a strong function of the positions of the molecules.

The trial free energy  $F_h$  is a function of the parameters fixing lattice dimensions and distortions through the constant term  $E_0$ . At a given temperature the structural configuration of the crystal will be the one specified by values of these parameters for which the free energy  $F_h$  is a minimum. Let  $\{n_i\}$  be the set of crystal parameters. Then their value at a given temperature can be determined from the conditions

$$\frac{\partial F_h}{\partial n_i} = 0. \quad (5.15)$$

Of particular interest in this work is the value of the lattice constant which can be obtained by solving Eq. (5.15) with  $n_i = a_0$ .

Equations (5.8), (5.14), and (5.15) are the basic equations of the quasiharmonic approximation and hold for any temperature  $T$ . In this work, however, only  $T=0$  was considered and henceforth the discussion will be restricted to this special case.

## VI. CALCULATIONS

The quasiharmonic equations are used in the following way. First, values of the structural parameters  $n_i$  are assumed and the force constants  $\Phi_{\alpha\beta}$  and  $\Phi_{\alpha\beta\gamma\delta}$  are generated from the molecular pair potentials. Initial values of the trial force constants  $\Gamma_{\alpha\beta}$  are then chosen; the harmonic constants  $\Phi_{\alpha\beta}$  serve as a good starting point. Dynamical matrices are constructed from the  $\Gamma_{\alpha\beta}$  and diagonalized to obtain the eigenvalues and eigenvectors. The correlation functions are then evaluated using Eq. (5.8) and inserted into Eq. (5.14) to obtain new values for the trial force constants. These are compared with the values used initially, and if the two sets do not agree within the desired accuracy, the process is repeated until convergence is obtained. The choice of  $n_i$  can then be checked using Eq. (5.15). If  $F_h$  is not stationary with respect to variation of  $n_i$ , another value is chosen and the procedure outlined above is repeated.

TABLE II. Frequencies after four iterations of the quasiharmonic calculation. Frequencies are listed in units  $\text{cm}^{-1}$ . Parameters:  $s = 0, 0$ ;  $b = 0$ ;  $\sigma = 3.6386 \text{ \AA}$ ;  $\epsilon = 1.6341 \times 10^{-14} \text{ erg}$ ;  $a_0 = 5.59 \text{ \AA}$ .

Cycle 1 harmonic	Cycle 2	Cycle 3	Cycle 4
42.63	41.52	41.46	41.46
52.50	53.89	53.83	53.83
55.16	57.28	56.96	56.96
56.06	59.51	59.14	59.19
63.12	65.62	65.19	65.25
79.21	84.78	84.36	84.36
93.38	90.14	89.83	89.83

In the numerical calculations the real space sums containing intermolecular pair potentials or their second derivatives were truncated after tenth neighbors. This was sufficient to ensure convergence, with the inclusion of additional neighbors causing the computed frequencies to vary by less than 0.3%. Only quartic interactions between first and second neighbors were included; the sum in Eq. (5.11) was thus restricted to terms involving 80 independent correlation functions. Likewise, only 80 of the quasiharmonic force constants differed from the harmonic ones.

The sums in Eqs. (5.8) and (5.3) over the Brillouin zone were replaced by integrals. The integrands were rewritten so as to have the point-group symmetry of the crystal, and the complete integrals were reduced to ones over the irreducible volume of the zone. These were evaluated numerically by Gaussian quadrature with a mesh of 76 points. A check calculation with a mesh of 119 points gave a value of the zero-point energy which was identical to that previously obtained to five significant figures.

Diagonalization of all dynamical matrices was done with EISPACK routines available from Argonne National Laboratory. The calculations for this study were performed on the CDC6500 at Purdue University. Iteration of the quasiharmonic calculation to convergence for a given potential required approximately 17 min with the FORTRAN programs used.

The quasiharmonic force constants obtained after the first iteration differed from the harmonic constants by as much as 10%; frequencies for  $\vec{k} = 0$  calculated with the new constants differed from the harmonic ones by 1 to 7%. Iterations were repeated until two consecutive sets of force constants differed by less than 1 part in 1000. In practice convergence was achieved after two iterations with the third set of quasiharmonic force constants. Table II lists the lattice frequencies for  $\vec{k} = 0$  calculated during each iteration of the

quasiharmonic calculation for four successive iterations.

## VII. POTENTIAL PARAMETERS AND LATTICE FREQUENCIES

Values of the optimum potential parameters were obtained by requiring that calculations of the crystal cohesive energy and the equilibrium lattice constant reproduce the experimental data exactly and that the spectral frequencies for  $\vec{k} = 0$  fit the measured values in the best least-squares sense. The data that were fitted are listed in Table III along with the values of other quantities used in the calculations.

### A. Harmonic approximation

A series of preliminary calculations using the harmonic approximation were performed to determine which values of the parameters to investigate. In these calculations the effect of the zero-point energy on the equilibrium lattice spacing and the  $P2_13$  distortion was ignored, and it was assumed that the values of the structural parameters minimized the static crystal energy. The static energy is an even function of the  $P2_13$  distortion  $s$ , with a positive curvature for  $s = 0$ , so in the approximation no distortion is predicted, and  $s$  was taken as zero for the subsequent harmonic calculations. The quadrupole moment  $Q$  was replaced as a potential parameter by the reduced quadrupole moment  $q$ ,

$$q = Q^2 / \epsilon (a_0^{\text{exp}})^5,$$

so that the static crystal energy was proportional to the Lennard-Jones parameter  $\epsilon$ . The parameter  $\sigma$  was then adjusted to make the unitless static energy  $\Phi_0^*$  assume its minimum value at the experimentally observed lattice spacing  $a_0^{\text{exp}}$ , for constant values of  $q$  and the bond length  $b$ . The unitless zero-point energy  $E_{zp}^*$  was calculated using Baldereschi's mean-value approximation technique<sup>35</sup> and  $\epsilon$  was determined from the equation

$$\epsilon \Phi_0^* + \epsilon^{1/2} E_{zp}^* = E_c, \quad (7.1)$$

where  $E_c$  is the measured cohesive energy. This procedure was followed for values of the bond length ranging from zero to the mean-internuclear separation and for values of the reduced quadrupole moment ranging between 0 and 0.12. The frequencies at  $\vec{k} = 0$  were calculated, and for each set of potential parameters the "goodness of fit"  $\Delta$ , defined as the square root of the sum of the squared deviations of the frequencies from the experimental values, was evaluated. A careful study of the results revealed that the best fit to the frequency spectra was obtained for a bond length equal to zero and a reduced quadrupole moment around 0.04. Figure 3 contains a plot of the



TABLE III. Values of molecular parameters and experimental data for  $\alpha$ -CO.

Quantity	Symbol	Value	Reference
Lattice constant	$a_0$	5.64 Å	a
Cohesive energy	$E_c$	1905 cal/mole	b
Frequencies	$A$	64.5 cm <sup>-1</sup>	c
	$E_T$	58 cm <sup>-1</sup>	c
	$E_L$	44 cm <sup>-1</sup>	c
	$T_T$	51.0 cm <sup>-1</sup>	d
	$T_T$	85 cm <sup>-1</sup>	d
	$T_L$	52 cm <sup>-1</sup>	c
	$T_L$	90.5 cm <sup>-1</sup>	c
Molecular mass	$M$	$4.6479 \times 10^{-23}$ g	d
Moment of inertia	$I$	$1.449 \times 10^{-39}$ g cm <sup>2</sup>	e
Mean internuclear separation		1.128 Å	e
c, m, -center-of-force distance	$g$	$8.0571 \times 10^{-2}$ Å	calc.
c, m, -O distance	$d$	$4.83429 \times 10^{-1}$ Å	calc.
$P2_13$ distortion	$s$	0.12 Å	f

<sup>a</sup>Crystal Data Determination Tables (American Crystallographic Association, New York, 1963).

<sup>b</sup>K. K. Kelley, Bull. U. S. Bur. Mines 383, 34 (1935).

<sup>c</sup>A. Anderson, T. S. Sun, and M. C. A. Donkersloot, Can. J. Phys. 48, 2265 (1970).

<sup>d</sup>A. Ron and O. Schnepp, J. Chem. Phys. 46, 3991 (1967).

<sup>e</sup>G. Herzberg, Spectra of Diatomic Molecules (Nostrand, New York, 1950).

<sup>f</sup>L. Vegard, Z. Phys. (Leipz.) 61, 185 (1930).

frequencies for zero bond length and  $0.04 \leq q \leq 0.05$ . In this graph a linear dependence on  $q$  has been assumed between the value 0.04 and 0.05, for which frequencies were calculated. The experimental values are indicated on the vertical axis. The vertical dashed line at  $q = 0.0401$  is the point at which  $\Delta$  is minimum. The second column of Table IV gives the interpolated frequency values, and Table V contains the optimum potential parameters.

#### B. Refinement of the harmonic approximation

When the effect of the varying zero-point energy was included in a calculation of the lattice constant, it was found that the harmonic potential defined by the parameters listed in Table V gave an equilibrium lattice spacing of 5.77 Å. The total energy was also found to have its minimum for a small but nonzero  $P2_13$  distortion, at  $s = -0.003$  Å. The sign indicates that the shift was in a direction opposite to that which was experimentally observed by Vegard, bringing the centers of mass of the CO molecules toward the  $Pa3$  lattice site. The change in  $s$  was too small to affect the determination of the potential parameters greatly and was thus neglected, but the parameters were readjusted in the following way to give the correct lattice spacing. For a given  $q$ , at least two values of  $\sigma$  were chosen and  $\Phi_0^*$  and  $E_{2b}^*$  were calculated for a minimum of three values of the lattice constant. Using Eq. (7.1)  $\epsilon(\sigma, q)$  was determined by

requiring that the total energy at  $a_0 = 5.64$  Å equal the experimentally measured cohesive energy. With this  $q$ ,  $\sigma$ ,  $\epsilon$  the crystal energy was determined as a function of the lattice parameter for each  $q$ ,  $\sigma$  from a parabola fitted to the computed values. For each  $q$ , the value of  $\sigma$  that made this minimum occur at the observed lattice spacing

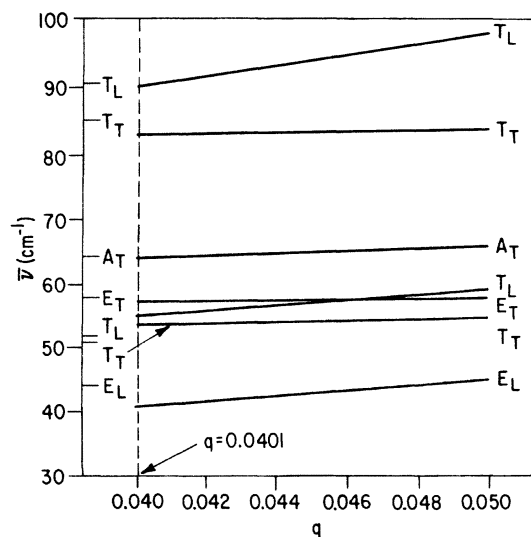


FIG. 3. Lattice frequencies as a function of the reduced quadrupole moment  $q$  for effective bond length  $b = 0.0$  Å: harmonic approximation.

TABLE IV. Calculated and observed lattice frequencies at  $\vec{k}=0$  for  $\alpha$ -CO. Numbers are in  $\text{cm}^{-1}$ . Units of  $\Delta$  are  $10^{12}$  rad/sec.

Mode	Harmonic $b=0$	Harmonic (refined) $b=0$	Harmonic (refined) $b=0.282 \text{ \AA}$	Quasi- harmonic $b=0$	Quasi- harmonic $b=0.282 \text{ \AA}$	ASD <sup>a</sup>	GH <sup>b</sup>	D <sup>c</sup>	PS <sup>d</sup>	SE <sup>e</sup>	Expt.
A	64.1	59.3	58.4	62.5	61.7	61					64.5
$E_T$	56.9	51.4	51.6	55.9	56.3	52					58
$E_L$	41.2	41.8	41.9	42.3	42.2	42.4	72	69.6			44
$T_T$	54.7	48.4	48.1	53.1	52.9	51			48	53	51
$T_L$	53.8	53.3	55.4	55.5	55.6	54.8	88	84.6			52
$T_T$	82.1	73.5	72.8	80.6	80.2	83			69	80	85
$T_L$	90.2	92.1	92.2	90.7	90.7	89.9	132	125.2			90.5
$\Delta$	1.113	2.843	3.011	1.299	1.379						

<sup>a</sup>A. Anderson, T. S. Sun, and M. C. A. Donkersloot, *Can. J. Phys.* **48**, 2265 (1970).

<sup>b</sup>D. A. Goodings and M. Henkelman, *Can. J. Phys.* **49**, 2898 (1971).

<sup>c</sup>P. V. Dunmore, *J. Chem. Phys.* **57**, 3348 (1972).

<sup>d</sup>A. Ron and O. Schnepp, *J. Chem. Phys.* **46**, 3991 (1967).

<sup>e</sup>T. Shinoda and H. Enokido, *J. Phys. Soc. Jpn.* **26**, 1353 (1969).

was found by interpolation. This, and the corresponding  $\epsilon$ , were the values of  $\sigma(q)$  and  $\epsilon(q)$  required to make the harmonic calculation reproduce the observed cohesive energy and lattice spacing. This process was followed for  $q=0.04$  and  $0.05$ , and bond lengths  $0$  and  $0.282 \text{ \AA}$ , and the  $\vec{k}=0$  frequencies calculated from the resultant potentials are plotted in Figs. 4 and 5. The best  $q$  values for the harmonic approximation were found by the least-squares procedure described before. Table IV contains the interpolated frequencies for these  $q$  and the corresponding potential parameters are listed in Table V. The agreement with experiment is definitely worse than that exhibited in Fig. 3,

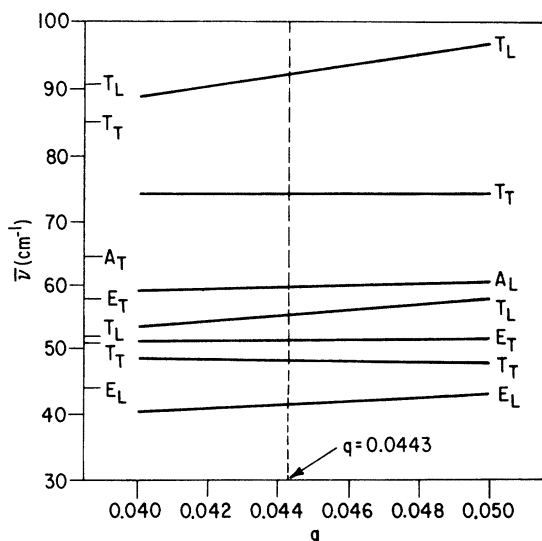


FIG. 4. Lattice frequencies as a function of the reduced quadrupole moment  $q$  for effective bond length  $b=0.0 \text{ \AA}$ : harmonic approximation (refined).

but that earlier agreement must be regarded as fortuitous, since it was obtained by a calculation with a potential that would not lead to the observed lattice constant.

TABLE V. Potential parameters for  $\alpha$ -CO.

	$\sigma$ ( $\text{\AA}$ )	$\epsilon$ ( $10^{-14}$ erg)	$Q$ (magnitude) ( $10^{-26}$ esu)
Harmonic $b=0$	3.7136	1.507	1.856
Harmonic (refined) $b=0$	3.6681	1.447	1.913
Harmonic (refined) $b=0.282 \text{ \AA}$	3.6331	1.491	1.913
Quasi- harmonic $b=0$	3.6791	1.428	1.980
Quasi- harmonic $b=0.282 \text{ \AA}$	3.6368	1.472	1.961
	3.702 <sup>a</sup>	1.195 <sup>a</sup>	2.43 <sup>a</sup>
	3.77 <sup>b</sup>	1.382 <sup>b</sup>	1.71 <sup>b</sup>
	3.59 <sup>c</sup>	1.494 <sup>c</sup>	1.81 <sup>d</sup>
			2.5 <sup>e</sup>

<sup>a</sup>T. H. Spurling and E. A. Mason, *J. Chem. Phys.* **46**, 322 (1967).

<sup>b</sup>L. Jansen, A. Michels, and J. M. Lupton, *Physica (Utr.)* **20**, 1215 (1954); **20**, 1235 (1954).

<sup>c</sup>J. O. Hirschfelder, C. F. Curtiss, and R. B. Bird, *The Molecular Theory of Gases and Liquids* (Wiley, New York, 1954).

<sup>d</sup>R. K. Nesbet, *J. Chem. Phys.* **40**, 3619 (1964).

<sup>e</sup>D. E. Stogryn and A. P. Stogryn, *Mol. Phys.* **11**, 371 (1966).

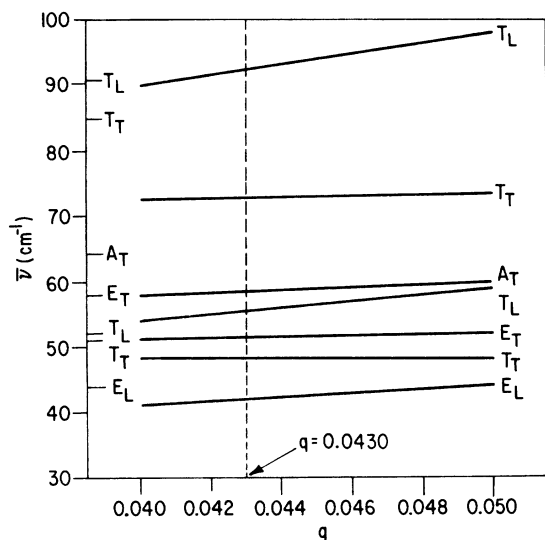


FIG. 5. Lattice frequencies as a function of the reduced quadrupole moment  $q$  for effective bond length  $b = 0.282 \text{ \AA}$ : harmonic approximation (refined).

### C. Quasiharmonic approximation

In view of the results for the harmonic approximation, the quasiharmonic calculation was performed for reduced quadrupole moments of 0.04 and 0.05 and effective bond lengths of 0 and 0.282 Å. In general, the  $P2_13$  distortion was assumed to be zero, but a single calculation with a nonzero value was performed to see whether the quartic potential was consistent with a distortion of the magnitude observed by Vegard. The general procedure for the computation was similar to that used in refining the harmonic model, except that the lattice frequencies corresponding to the optimum potential for a given  $q$  were determined with adequate accuracy by interpolation, along with  $\sigma$  and  $\epsilon$ . The adjustment of  $\epsilon$  to fit the cohesive energy was carried out as follows. In the quasiharmonic approximation, the crystal energy is given by

$$E_c = E_{zp} + E_0, \quad (7.2)$$

where  $E_{zp}$  is the zero-point energy calculated using the optimum trial harmonic force constants and  $E_0$ , as given in Eq. (5.11), is the difference between the averages of the anharmonic quartic potential and the trial harmonic potential over the trial ground-state wave function. The equation for  $E_0$  can be written

$$E_0 = \Phi_0 + \langle \Phi_2 \rangle - \langle \Gamma_2 \rangle + \langle \Phi_4 \rangle. \quad (7.3)$$

Here  $\Phi_0$  is the static energy,  $\Phi_2$  and  $\Phi_4$  are, respectively, the quadratic and quartic portions of the crystal potential, and  $\Gamma_2$  is the trial harmonic potential. Examination of Eq. (5.14) shows that

$\langle \Gamma_2 \rangle$  can be broken into two parts

$$\langle \Gamma_2 \rangle = \langle \Phi_2 \rangle + \langle \Gamma_{\text{cor}} \rangle, \quad (7.4)$$

where  $\langle \Gamma_{\text{cor}} \rangle$  arises from the quartic correction term in the equation. Thus Eq. (7.3) becomes

$$E_0 = \Phi_0 - \langle \Gamma_{\text{cor}} \rangle + \langle \Phi_4 \rangle. \quad (7.5)$$

The static energy is readily computed for a chosen potential. The results of the self-consistent calculation with the chosen potential include the corrections to the harmonic force constants and the correlation functions computed using the optimum trial Hamiltonian, which are used in evaluating the other terms.

For fixed  $q$  the static energy is proportional to  $\epsilon$ , and in an harmonic calculation the zero-point energy  $E_{zp}$  is proportional to  $\epsilon^{1/2}$ . The corrections to the harmonic force constants computed during the first iteration of the self-consistent calculation are proportional to  $\epsilon^{1/2}$ , since as given in Eq. (5.14) they are sums of products of quartic derivatives, which are proportional to  $\epsilon$ , and correlation functions, which are proportional to  $\omega^{-1}$  and therefore to  $\epsilon^{-1/2}$ . After this iteration these functional dependences do not strictly hold, since the quasiharmonic force constants have a term proportional to  $\epsilon^{1/2}$  as well as one proportional to  $\epsilon$ . The deviation, however, is very small, and in any case the crystal energy is dominated by  $\Phi_0$  which is strictly proportional to  $\epsilon$ . The average  $\langle \Gamma_{\text{cor}} \rangle$ , which contains products of force-constant corrections and two correlation functions, and similarly  $\langle \Gamma_4 \rangle$  are nearly independent of  $\epsilon$ . In a limited range of  $\epsilon$  the crystal energy can then be written

$$E_c \approx \epsilon \Phi_0^* + \epsilon^{1/2} E_{zp}^* - \langle \Gamma_{\text{cor}} \rangle^* + \langle \Phi_4 \rangle^*, \quad (7.6)$$

with the starred quantities treated as independent of  $\epsilon$ .

For fixed  $\sigma$  and  $q$  and the lattice constant at the measured value, the harmonic value for  $\epsilon$  was used in the first iteration; then  $E_{zp}^*$  and  $\langle \Phi_4 \rangle^*$  were calculated and  $\langle \Gamma_{\text{cor}} \rangle^*$  was set equal to zero. These values were substituted into Eq. (7.6) along with  $\Phi_0^*$  and  $E_c$ , and the equation was solved for  $\epsilon$ . This  $\epsilon$ , which differed from the harmonic result by approximately 2%, was used in the second iteration. The process was repeated, now with computed values of  $\langle \Gamma_{\text{cor}} \rangle^*$ , until  $\epsilon$  and the other quantities converged within the desired accuracy, generally after three iterations.

After  $\epsilon$  was determined in this fashion for fixed  $q$  and  $\sigma$ , the crystal energy was calculated in the quasiharmonic approximation for two other values of the lattice constant, and the remainder of the procedure followed that used for the harmonic approximation. The lattice frequencies for the two effective bond lengths are plotted in Figs. 6

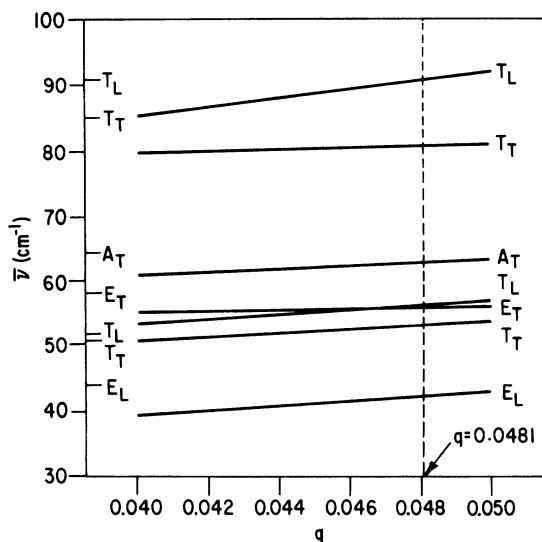


FIG. 6. Lattice frequencies as a function of the reduced quadrupole moment  $q$  for effective bond length  $b = 0.0 \text{ \AA}$ : quasiharmonic approximation.

and 7, and the frequencies for the optimum  $q$  are listed in Table IV. Table V contains the interpolated values of the best potential parameters.

The crystal energy was calculated in the quasiharmonic approximation for a  $P2_13$  distortion of  $0.05 \text{ \AA}$  and compared with that for zero distortion with all other parameters held constant. The energy for zero distortion was lower. If the quasiharmonic approximation predicts a distortion, therefore, it is less than  $0.025 \text{ \AA}$ , that is, less than 20% of that observed by Vegard, or is in the opposite direction.

The harmonic and quasiharmonic frequency spectra were calculated for the potential with parameters  $b = 0.0$ ,  $\epsilon = 1.4806 \times 10^{-14} \text{ erg}$ ,  $q = 0.04$ , and  $\sigma = 3.6636 \text{ \AA}$ . A comparison of the two showed that, for a given potential, the librational frequencies calculated in the quasiharmonic approximation are lower than those calculated in the harmonic approximation, and the translational frequencies higher.

## VIII. DISCUSSION AND CONCLUSIONS

### A. Potential parameters

Table V contains the optimum potential parameters that were found for the harmonic and quasiharmonic approximations, along with several previously calculated or measured values. Comparison of the results for the harmonic and refined harmonic calculations indicates that it is important to take account of the variation of the zero-point energy with the lattice constant. The best estimates of the potential parameters are the  $b = 0$  quasihar-

monic results. The quadrupole moment ( $1.980 \times 10^{-26} \text{ esu}$ ) is 20% lower than the recommended gas-phase value but is close to the values derived from crystal data ( $-1.71 \times 10^{-26} \text{ esu}$ ) and theoretical calculations ( $-1.81 \times 10^{-26} \text{ esu}$ ). The Lennard-Jones parameter  $\epsilon$  ( $1.428 \times 10^{-14} \text{ erg}$ ) is in agreement with the commonly used value ( $1.38 \times 10^{-14} \text{ erg}$ ). Comparison of the predicted spectra indicates that bond length  $b = 0$  is better than  $b = 0.282 \text{ \AA}$ , and the two-center model gives little improvement over the one-center Lennard-Jones model.

### B. Frequency spectrum

Table IV contains the calculated lattice frequencies for the harmonic and quasiharmonic approximations, with the experimental values and the results of other calculations included for comparison. The calculated librational frequencies are compared with those measured by Anderson *et al.* at 18 K. The studies of Cahill and Leroy<sup>38</sup> show that the corresponding frequencies for  $\alpha\text{-N}_2$  have some temperature dependence, with the peaks shifting toward lower values as the temperature increases, changing by  $3 \text{ cm}^{-1}$  between 16 and 34 K. There is, however, insufficient data available for an extrapolation of the librational frequencies of  $\alpha\text{-CO}$  to  $T = 0$ , and the experimental results of Anderson *et al.* were used without any corrections for temperature dependence.

The first harmonic calculation with zero bond length discussed here is very similar to the model of Anderson *et al.*, and it is not surprising that the calculated spectra are very close. Differences between the two can be attributed to differ-

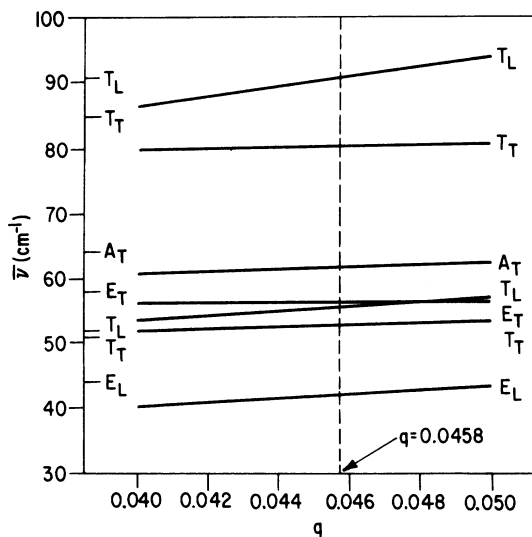


FIG. 7. Lattice frequencies as a function of the reduced quadrupole moment  $q$  for effective bond length  $b = 0.282 \text{ \AA}$ : quasiharmonic approximation.

ences in the potential parameters, and to the fact that the inequivalence of the center of force and center of mass is included here; this results primarily in a larger separation of the doubly degenerate  $E$  modes, each being shifted by  $\sim 2\%$ .

Examination of Figs. 4 and 6 and Figs. 5 and 7 shows that the frequencies calculated in the quasi-harmonic approximation for the two bond lengths give a much better fit to the observed spectrum than the corresponding (refined) harmonic approximation results. The fit parameters  $\Delta$  provide a numerical measure of the improved agreement: the harmonic  $\Delta$  values ( $2.843 \times 10^{12}$  and  $3.011 \times 10^{12}$  rad/sec) are larger than the quasi-harmonic values ( $1.299 \times 10^{12}$  and  $1.379 \times 10^{12}$  rad/sec) by more than a factor of 2. The difference between one-center and two-center fits for a given approximation is not large, although the one-center fits are better, i. e., in the quasi-harmonic approximation the one-center potential gives  $\Delta = 2.843 \times 10^{12}$  rad/sec and the two-center,  $\Delta = 3.011 \times 10^{12}$  rad/sec. The best potential parameters, listed in the fourth row of Table V, give average errors of 4.0 and 3.6% for the translational and librational frequencies, respectively. The maximum error (6.7%) occurs for the low-frequency triply-degenerate librational mode.

The librational frequencies depend strongly on the assumed value for the quadrupole moment  $Q$ . If Goodings and Henkelman and Dunmore had used a value for  $Q$  in the range that this work indicates is appropriate for  $\alpha$ -CO, instead of the recommended gas-phase value, which is definitely too high, their computed frequencies would agree reasonably well with the observed ones.

The effect of the approximation used to obtain the librational kinetic energy on the calculated spectrum is unclear. If the correction to the kinetic energy for singly excited states is of the same size and in the same direction as the correction for the ground state, there will be little change in the tabulated spectrum. On the other hand, the

corrections may not cancel; this needs to be investigated in more detail.

### C. Mass dissymmetry

For values of the reduced quadrupole moment in the range suitable for  $\alpha$ -CO, the displaced center of mass affects the calculated frequency spectrum only slightly for zero effective bond length. The  $A$  mode frequency is unchanged, since the direction of motion of each molecule is along the line joining the center of force and the center of mass, with no tendency toward libration about the center of mass. Of the triply degenerate  $T$  modes, the most affected is the highest, which is raised by 1.3%. The  $E$  modes exhibit the most sensitivity, being raised or lowered by 2.3%.

The character of the modes is affected, and mixing of translational and librational symmetry coordinates occurs. For the  $q$  values of interest, however, the modes can still be classified as predominantly translational or librational. For any given  $T$  mode the minor component does not exceed 6% of the total for  $q = 0.05$ . For the  $E$  modes this is 14% in the harmonic approximation and 18% in the quasi-harmonic approximation.

### D. $P_{2,3}$ distortion

Both the intermolecular potentials used here and the quasi-harmonic approximation fail to predict a  $P_{2,3}$  distortion of the size and in the direction of that observed by Vegard. It is also clear that the mass dissymmetry does not give rise to the distortion in  $\alpha$ -CO, since the same type of distortion is reported in  $\alpha$ -N<sub>2</sub>, which is composed of symmetric molecules. It appears from these results that an explanation of the structure of  $\alpha$ -CO and  $\alpha$ -N<sub>2</sub> must be sought elsewhere.

### ACKNOWLEDGMENT

We gratefully acknowledge the support of the National Science Foundation.

\*Based on a thesis presented by Barbara Okray Hall in partial fulfillment of the requirements for the degree of Doctor of Philosophy at Purdue University, (1974). Supported in part by a grant from the NSF.

†Argonne National Laboratory, Argonne, Illinois.

<sup>1</sup>L. Pauling, Phys. Rev. **36**, 430 (1930).

<sup>2</sup>B. C. Kohin, J. Chem. Phys. **33**, 882 (1960).

<sup>3</sup>J. C. Raich, J. Chem. Phys. **56**, 2395 (1972).

<sup>4</sup>N. Jacobi and O. Schnepp, J. Chem. Phys. **57**, 2516 (1972).

<sup>5</sup>A. Anderson, T. S. Sun, and M. C. A. Donkersloot, Can. J. Phys. **48**, 2265 (1970).

<sup>6</sup>D. A. Goodings and M. Henkelman, Can. J. Phys. **49**, 2898 (1971).

<sup>7</sup>T. Shinoda and H. Enokido, J. Phys. Soc. Jpn. **26**,

1353 (1969).

<sup>8</sup>T. S. Kuan, A. Warshel, and O. Schnepp, J. Chem. Phys. **52**, 3012 (1970).

<sup>9</sup>O. Schnepp and A. Ron, Discuss. Faraday Soc. **48**, 26 (1969).

<sup>10</sup>L. Vegard, Z. Phys. (Leipzig) **61**, 185 (1930).

<sup>11</sup>R. K. Nesbet, J. Chem. Phys. **40**, 3619 (1964).

<sup>12</sup>R. F. W. Bader, W. H. Henneker, and P. E. Cade, J. Chem. Phys. **46**, 3341 (1967).

<sup>13</sup>C. A. Burrus, J. Chem. Phys. **28**, 427 (1958).

<sup>14</sup>M. W. Melhuish and R. L. Scott, J. Phys. Chem. **68**, 2301 (1964).

<sup>15</sup>R. F. Curl, H. P. Hopkins, and K. S. Pitzer, J. Chem. Phys. **48**, 4064 (1968).

<sup>16</sup>E. K. Gill and J. A. Morrison, J. Chem. Phys. **45**,

- 1585 (1966).
- <sup>17</sup>J. O. Clayton and W. F. Giaque, *J. Am. Chem. Soc.* 54, 2610 (1932).
- <sup>18</sup>D. R. Williams, L. J. Schaad, and J. N. Murrell, *J. Chem. Phys.* 47, 12 (1967).
- <sup>19</sup>J. C. Raich and R. D. Etters, *Phys. Rev.* 168, 425 (1968).
- <sup>20</sup>C. F. Coll, III, and A. B. Harris, *Phys. Rev. B* 2, 1176 (1970).
- <sup>21</sup>P. V. Dunmore, *J. Chem. Phys.* 57, 3348 (1972).
- <sup>22</sup>S. H. Walmsley and J. A. Pople, *Mol. Phys.* 8, 345 (1964).
- <sup>23</sup>H. Montgomery and G. Dolling, *J. Chem. Phys. Solids* 33, 1201 (1972).
- <sup>24</sup>A. A. Maradudin, E. W. Montroll, G. H. Weiss, and I. P. Ipatova, *Theory of Lattice Dynamics in the Harmonic Approximation*, 2nd ed. (Academic, New York, 1971).
- <sup>25</sup>T. R. Koehler, *Phys. Rev.* 139, A1097 (1965).
- <sup>26</sup>T. R. Koehler, *Phys. Rev.* 141, 281 (1966).
- <sup>27</sup>T. R. Koehler, *Phys. Rev.* 144, 789 (1966).
- <sup>28</sup>N. R. Werthamer, *Am. J. Phys.* 37, 763 (1969).
- <sup>29</sup>N. R. Werthamer, *Phys. Rev. B* 1, 572 (1970).
- <sup>30</sup>S. Doniach, in *Lattice Dynamics*, edited by R. F. Wallis (Pergamon, Oxford, 1965), pp. 305–310.
- <sup>31</sup>D. J. Hooton, *Philos. Mag.* 46, 422 (1955).
- <sup>32</sup>N. Boccara and G. Sarma, *Physics* 1, 219 (1965).
- <sup>33</sup>P. F. Choquard, *The Anharmonic Crystal* (Benjamin, New York, 1967).
- <sup>34</sup>R. P. Feynman, *Statistical Mechanics* (Benjamin, Reading, Mass., 1972), p. 67.
- <sup>35</sup>A. Baldereschi, *Phys. Rev. B* 7, 5212 (1973).
- <sup>36</sup>J. E. Cahill and G. E. Leroi, *J. Chem. Phys.* 51, 1324 (1969).